JMM

Analysis of a May-Holling-Tanner rate-dependent predator-prey model with an alternative food source for the predator with a weak Allee effect for the prey

Marco Antonio Romero-Ordoñez[†][*], Jhelly Reynaluz Pérez-Núñez[†], Neisser Pino-Romero[§]

[†]*Departamento Académico de Matemáticas, Facultad de Ciencias Matemáticas, Universidad Nacional Mayor de San Marcos, Lima, Perú*
[§]*Departamento Académico de Ciencias Exactas, Facultad de Ciencias e Ingeniería, Universidad Peruana Cayetano Heredia, Lima, Perú*
Email(s): marco.romero7@unmsm.edu.pe, jhelly.perez@unmsm.edu.pe, neisser.pino@upch.pe

Abstract. In this study, a May-Holling-Tanner-type mathematical model of the predator-prey interaction is analyzed, incorporating an alternative food source for the predator and a weak Allee effect on the prey population. The model is described using a two-dimensional system of ordinary differential equations. The existence, uniqueness, and positivity of the solutions were investigated, ensuring that the populations were maintained at biologically meaningful values. Furthermore, local and global stability conditions at critical points suitable for ecological equilibrium are explored using tools such as the generalized Krasovskii theorem. Likewise, the existence of periodic solutions in certain scenarios is based on the Dulac criterion. Finally, a numerical analysis using Python simulations is performed to corroborate the theoretical results, highlighting the asymptotic stability of the populations under certain initial and parameter conditions.

Keywords: Mathematical ecology, weak Allee effect, LaSalle, generalized Krasovskii, Dulac's criterion
AMS Subject Classification 2010: 34A34, 65L05.

1 Introduction

A mathematical model is a formal abstraction designed to represent a phenomenon or the interdependence between two or more variables, articulated through mathematical equations, functions, or formulas. Such models serve as invaluable tools for analyzing complex relationships and are widely employed to understand phenomena across natural, social, and physical sciences. Depending on the purpose and structure of the model, they can also be utilized to forecast future values of the system's variables with significant precision. In ecological and biological research, one of the most powerful approaches

for analyzing and predicting system behavior is the formulation and subsequent simulation of mathematical models. The current prominence of mathematical modeling in these fields is driven by an enhanced understanding of biological mechanisms, coupled with significant advancements in computational technologies and mathematical software. Pioneers like Thomas Malthus (1798) [39], Pierre Verhulst (1838) [55], Alfred Lotka (1925) [35], Vito Volterra (1926) [57], and Patrick Leslie (1948) [30] laid the foundational groundwork for mathematical approaches in biological systems, providing critical insights into population dynamics and ecological interactions. A noteworthy concept in this domain is the Allee effect, named after Warder Clyde Allee, an American ecologist who extensively studied the advantages of cooperative behaviors in small populations [2,3]. Stephens et al. [52] formally defined the Allee effect as a positive correlation between an individual's fitness and the population density or size. In other words, an individual's fitness diminishes as the population size decreases, highlighting the challenges faced by small populations in maintaining viability. For additional information, refer to [27,52]. This phenomenon has been described using various terminologies, including "dispensation","negative competition effect", "inverse density dependence", "positive density dependence", "underpopulation," and "allelocatalytic." The term "dispensation" is predominantly employed in fisheries science, while the "Allee effect" is more widely recognized and utilized in the disciplines of biology and ecology [32]. The Allee effect is typically categorized into two distinct types: the component Allee effect and the demographic Allee effect. The component Allee effect refers to a positive correlation between any specific measure of individual fitness—such as reproductive success or survival probability—and population density. In contrast, the demographic Allee effect encompasses a more generalized positive relationship between overall individual fitness and population density, reflecting how small populations can face challenges in achieving growth and long-term sustainability.

The presence of a demographic Allee effect inherently implies the existence of at least one component Allee effect; however, the reverse is not necessarily true. From an ecological standpoint, the demographic Allee effect can be further classified into two forms: the strong Allee effect and the weak Allee effect. The key distinction lies in the population's per capita growth rate. While populations experiencing a weak Allee effect may have low densities, they consistently maintain a positive per capita growth rate, enabling them to recover under favorable conditions. Conversely, populations subject to a strong Allee effect exhibit a critical density threshold below which the per capita growth rate becomes negative, significantly increasing their risk of extinction. In summary, populations with a weak Allee effect are more resilient and less prone to extinction compared to those experiencing a strong Allee effect [15].

The Allee effect manifests in various populations due to a range of biological factors, including diminished predator vigilance, impaired social thermoregulation, difficulties in finding mates, and suboptimal foraging efficiency at low population densities. Additional contributing factors have also been identified and systematically categorized. For a detailed summary, refer to Table 1 in [11] and Table 2.1 in [15]. The differential equation frequently employed to model this phenomenon is expressed as:

$$\frac{dx}{dt} = rx\left(1 - \frac{x}{k}\right)(x - m) \tag{1}$$

In the following, we present notable precedents for the application of the weak Allee effect in ecological mathematical models. These examples are not necessarily aligned with the methodological framework employed in this work but illustrate the versatility of the weak Allee effect in various ecological contexts. In [8], the influence of stochastic noise on the carrying capacity of the prey population is analyzed, focusing on the dynamics of the Truscott-Brindley system, which models interactions between phytoplankton and zooplankton under a weak Allee effect. In [16,60], a non-autonomous Lotka-Volterra multispecies competitive system is investigated, incorporating delays and the weak Allee effect. In [37],

the dynamics of a delay-based food chain system are studied, where a weak Allee effect and a refuge for intermediate predators are included. Similarly, [62] examines a stochastic predator-prey model with a Holling-(n+1) functional response, incorporating the weak Allee effect as a central mechanism. The study in [9] explores an eco-epidemiological model that describes the interactions between susceptible prey, infected prey, and predators, considering the impacts of both the Allee effect and random disturbances. Additionally, [46] develops a mathematical model to analyze an eco-epidemiological system in which the prey population is affected by a disease, focusing on the combined effects of incubation delays and the weak Allee effect on predator population dynamics. Lastly, [61] investigates two-dimensional bifurcations and their control mechanisms in a predator-prey system, emphasizing the role of the weak Allee effect on prey population dynamics.

In [59], the dynamic behavior of a reaction-diffusion-advection model incorporating weak Allee effect-type growth is analyzed. This study emphasizes the role of spatial processes in systems exhibiting Allee dynamics. In [53], the weak Allee effect is integrated into the prey equation of a predator-prey model, and the conditions under which Hopf bifurcations occur are derived, providing insights into the oscillatory dynamics of such systems. The study in [58] investigates an invasion model based on a reaction-diffusion framework that accounts for a complete spectrum of Allee effects, including the weak Allee effect, offering a comprehensive analysis of spatial invasion dynamics. In [33], a predator-prey model featuring a non-monotonic functional response and a weak Allee effect on the prey population is presented. The global dynamics of the system are rigorously analyzed through a combination of qualitative techniques and bifurcation analysis, providing a deep understanding of the system's behavior under varying conditions. In [47], a general prey-predator model is proposed where both prey and predator populations are affected by weak Allee effects and prey diseases. The study provides a thorough examination of the basic dynamical properties of the full model as well as submodels, with and without the Allee effect. Furthermore, [26] explores the Leslie-Gower predator-prey model incorporating a weak Allee effect. The analysis begins by addressing the existence and stability of nonnegative equilibria and subsequently investigates various bifurcation phenomena in positive equilibria, including saddle-node bifurcation, Hopf bifurcation, and Bogdanov-Takens bifurcation, thereby highlighting the rich dynamical behavior of the system.

Some notable precedents for the application of the weak Allee effect, relevant to this line of research, are summarized as follows. In [56], a Leslie-Gower predation model is analyzed, where predator consumption is described by a sigmoidal functional response. The prey population is subject to an Allee effect, and predators are treated as generalists, highlighting the interplay between functional responses and prey population thresholds. In [19], the impact of cooperative hunting among predators on prey populations, which are affected by a weak Allee effect, is explored. The study examines how predator collaboration influences the persistence and stability of prey populations. The work in [63] focuses on the number and stability of oscillations in a slow-fast predator-prey system incorporating a weak Allee effect and a Holling-IV functional response, revealing complex dynamics such as relaxation oscillations and multi-scale behaviors. Additionally, [36] investigates a Beddington-DeAngelis amensalism system, where one species experiences a weak Allee effect while the other inhibits its growth and survival without being affected itself. This study sheds light on the interplay between antagonistic interactions and population thresholds. In [18], the role of memory and the weak Allee effect in the coexistence of two interacting species is examined, with a focus on the system's stability properties and ecological implications. The study in [31] addresses the effects of sterile insect technique (SIT) on mosquito populations by developing a mathematical model involving the constant release of sterile Aedes aegypti mosquitoes. Both strong and weak Allee effects are incorporated, along with interspecific competition with Anopheles

mosquitoes, to evaluate the effectiveness of SIT in population control. Finally, [34] presents a Leslie-Gower model that incorporates the weak Allee effect on prey and the fear effect on predators. This model is analyzed under two scenarios: with and without the fear effect, providing insights into how predator behavioral responses influence population dynamics.

In [49], a rate-dependent predator-prey model incorporating prey disease is developed, where survival thresholds for susceptible prey under both strong and weak Allee effects are considered. Predator-prey models are typically classified based on the nature of their functional response, which can be dependent solely on the prey population size or a mixed functional response, dependent on both prey and predator population sizes. Functional responses such as Holling types I, II, III, and IV are categorized in the first group [40, 54], as these models describe how the predator's rate of capture, consumption, and conversion of prey into new predator offspring depends on the availability of prey in the environment shared by both species.

However, these traditional predator-prey models have faced criticism from several ecologists and biologists—such as Arditi, Akcakaya, Gutierrez, and Cosner [1, 4, 5, 7, 20]—due to their limited ability to accurately capture predator-prey interactions. Such criticisms are supported by substantial biological evidence, as discussed in [4, 21]. In response, Arditi and Ginzburg [4] introduced a mixed functional response, termed rate-dependent, which aims to modify non-mixed functional responses into mixed ones, transforming the response function from $h(x)$ to $h(\frac{x}{y})$, where x represents the prey population and y represents the predator population. Furthermore, the rate-dependent functional response is not the only mixed response model; others include the Beddington-DeAngelis, Crowley-Martin, and Hassel-Varley functional responses. Among these, the rate-dependent functional response applied to the Holling type II prey-dependent response provides a more biologically accurate representation of predator-prey dynamics compared to the models discussed above.

In this paper, we propose to incorporate the weak Allee effect into the model presented in [45] to investigate its implications. Specifically, the weak Allee effect is introduced into a predator-prey mathematical framework, which is represented by the May-Holling-Tanner model featuring a mixed rate-dependent functional response and alternative food sources for the predator. This combination of factors models an ecosystem consisting of a prey species, which serves as the preferred food for a predator species, where the growth of the prey population is constrained by the availability of resources in the ecosystem. Moreover, there exists a positive correlation between the prey growth rate and population size at low densities. In this setting, cooperative behaviors, such as social interactions, are vital for the growth of the prey population at low densities. Finally, the predator population growth is regulated by the availability of prey, with the inclusion of alternative food sources for the predator.

The present study is organized into nine sections, including an introduction, summary, and references. The first section, Mathematical Model, introduces the differential equation (ODE) system under investigation, outlining the biological significance of each variable and parameter used. The following section, Positivity and Boundedness, ensures that the solutions of the system remain within biologically meaningful limits, meaning that the populations do not grow infinitely but are instead bounded. In the next section, Topological Equivalence, a simplified system equivalent to the original one is presented. This equivalent system is more analytically tractable, and hence, it will be the focus of further analysis. The subsequent section explores the critical points of the equivalent system, confirming that these points are positive and thus biologically relevant. A local stability analysis suitable for ecological equilibrium is applied to the critical points, which tries to cause that every solution close to the critical points is attracted to the same critical points, however, we want to cause that every solution included in the region associated to the system under study is attracted to the critical points that are comprised by the region

in question, for this it is demonstrated that this region is asymptotically stable and does not contain periodical solutions.

This is followed by the section Numerical Analysis, where simulations are conducted and interpreted biologically to provide insights into ecological equilibrium. Finally, the Conclusions section summarizes the findings from each previous section, offering an overview of the model's implications, potential applications, future research directions, and limitations.

2   Mathematical Model

The system of autonomous two-dimensional ordinary differential equations is given by the following:

$$
X_\sigma(x,y) : \begin{cases} \dfrac{dx}{dt} = rx\left(1 - \dfrac{x}{k}\right)(x-m) - \dfrac{qxy}{x+ay}, \\[4mm] \dfrac{dy}{dt} = y\left(1 - \dfrac{y}{nx+c}\right)s, \end{cases}
\tag{2}
$$

where x and y denote the number of prey and the number of predators at time t. In addition, r represents the intrinsic growth rate of the prey population. This parameter captures the prey's ability to grow under ideal conditions without external constraints, k denotes the carrying capacity of the prey population, which is the maximum population size that the environment can sustainably support, considering the available resources; m is called the minimum viable population or extinction threshold, q represents the intrinsic growth rate of the prey, and a is the degree to which the environment protects the prey. In addition, s represents the intrinsic growth rate of the predator, n measures the quality of the prey as food for the predator, and the parameter c describes the size of the alternative food for the predator. This prompts us to define the following vector $\sigma = (r,k,q,a,s,n,c,-m)$. For convenience, we have that $-m = m_1$. Thus, the system (2) is defined in the following region:

$$
\Omega = \left\{(x,y) \in \mathbb{R}^2 : 0 < x; 0 < y\right\}.
\tag{3}
$$

The proof of existence and uniqueness of solutions is provided in the following section.

3   Positivity, boundedness, existence, and uniqueness of solutions

Since we are working on an ecological-biological model, the following results show that the solutions in the system (2) are positive and do not grow indefinitely.

Definition 1. *Let $\Omega \subset \mathbb{R}^n$ and $x(t) \in \mathbb{R}^n$ be the solution of the system $\dfrac{dx(t)}{dt} = f(x)$. It is said that Ω is invariant for the system if $x(0) \in \Omega$, then $x(t) \in \Omega$ for all $t \geq 0$.*

Proposition 1. *The region Ω associated with the system (2) is invariant.*

Proof. Let

$$
\begin{cases}
\dfrac{dx(t)}{dt} = \left(r\left(1 - \dfrac{x(t)}{k}\right)(x(t)+m_1) - \dfrac{qy(t)}{x(t)+ay(t)} \right) x(t), \\[3mm]
\dfrac{dy(t)}{dt} = \left(s - \dfrac{sy(t)}{nx(t)+c} \right) y(t), \\[3mm]
x(0) > 0, \quad y(0) > 0,
\end{cases}
$$

be the initial value problem associated with the system (2) with initial point $(x(0), y(0)) \in \Omega$. By solving the above system, we obtain

$$
x(t) = x(0)\exp\left\{ \int_0^t \left(r\left(1 - \frac{x(\iota)}{k}\right)(x(\iota)+m_1) - \frac{qy(\iota)}{x(\iota)+ay(\iota)} \right) d\iota \right\} > 0,
$$

$$
y(t) = y(0)\exp\left\{ \int_0^t \left(s - \frac{sy(\iota)}{nx(\iota)+c} \right) d\iota \right\} > 0.
$$

Hence, we have $x(t) > 0$ and $y(t) > 0$. Therefore, $(x(t), y(t)) \in \Omega$, for all $t \geq 0$. Thus, we see that the region Ω associated with the system (2) is invariant. $\qquad\square$

Theorem 1. *The solutions $x(t)$ and $y(t)$ of the system (2) are bounded for all $t \geq 0$.*

Proof. From the first equation of the system (2), we have

$$
\frac{dx}{x(k-x)(x+m_1)} \leq \frac{r}{k}dt.
$$

By appropriately integrating and rearranging, we obtain:

$$
\frac{1}{m_1}\int_0^t \frac{dx(\iota)}{x(\iota)} - \frac{1}{k+m_1}\int_0^t \frac{d(k-x(\iota))}{k-x(\iota)} \leq r\int_0^t d\iota + \frac{k}{m_1(k+m_1)}\int_0^t \frac{1}{x(\iota)+m_1}dx(\iota).
$$

By applying the absolute value and the Minkowski inequality to the integrals, we obtain:

$$
\left| \frac{1}{m_1}\int_0^t \frac{dx(\iota)}{x(\iota)} - \frac{1}{k+m_1}\int_0^t \frac{d(k-x(\iota))}{k-x(\iota)} \right| \leq rt + \left| \frac{k}{m_1(k+m_1)} \right| \left| \int_0^t \left| \frac{1}{x(\iota)+m_1} \right| dx(\iota) \right.
$$

It is clear that if $m_1 < x(\iota) + m_1 < 1$, then $\dfrac{1}{x(\iota)+m_1} < \dfrac{1}{m_1}$ and if $x(\iota)+m_1 > 1$ then $\dfrac{1}{x(\iota)+m_1} < 1$.

Therefore $\left| \dfrac{1}{x(\iota)+m_1} \right| \leq A$ for all $\iota \in [0,t]$, where $A = \max\{1, \dfrac{1}{m_1}\}$. Furthermore, substituting into the equation yields:

$$
k\ln\left(\frac{x(t)}{x(0)}\right) + m_1\ln\left(\frac{x(t)(k-x(t))}{x(0)(k-x(0))}\right) \leq tMm_1(k+m_1),
$$

where $M = r + \frac{Ak}{m_1(k+m_1)}$. By incorporating the exponent, we obtain:

$$
\left(\frac{x(t)}{x(0)}\right)^k \left(\frac{x(t)(k-x(0))}{x(0)(k-x(t))}\right)^{m_1} \leq e^{(tMm_1k + tMm_1^2)}. \tag{4}
$$

For convenience, we separate Eq. (4) into Eqs. (5) and (6):

$$\left(\frac{x(t)}{x(0)}\right)^k \le e^{(tMm_1k)}, \tag{5}$$

$$\left(\frac{x(t)(k-x(0))}{x(0)(k-x(t))}\right)^{m_1} \le e^{(tMm_1^2)}, \tag{6}$$

Note that multiplying Eq. (5) by Eq. (6) yields Eq. (4). From Eq. (5), we obtain

$$x(t) \le x(0)e^{(tMm_1)}. \tag{7}$$

It follows from (6) that

$$x(t) \le \frac{kx(0)e^{(tMm_1)}}{k+x(0)(e^{(tMm_1)}-1)}. \tag{8}$$

Applying the limits to the results in Eqs. (7) and (8), we obtain, respectively, that:

$$\lim_{t\to\infty} x(t) \le \infty, \quad \lim_{t\to\infty} x(t) \le k.$$

Thus, $x(t) \le k$ for all $t \ge 0$. From the second equation of the system (2), we deduce that

$$\frac{dy}{y(nk+c-y)} \le \frac{sdt}{nk+c}.$$

By appropriately integrating and rearranging, we obtain

$$y(t) \le \frac{(nk+c)y(0)e^{(st)}}{nk+c+y(0)(e^{(st)}-1)}.$$

Applying the limits, it turns out that $y(t) \le n+c$ for all $t \ge 0$. $\qquad\square$

From the previous theorem, it follows that $0 < (x(t)+y(t)) \le k(n+1)+c$. In addition, the region of analysis is limited, that is,

$$\Omega = \{(x,y) \in \mathbb{R}^2 : 0 < x \le k; 0 < y \le nk+c\}.$$

This method of bounding the solutions contrasts with approaches in articles such as [25,44]. According to Corollary 2.2.3, as presented in [23] [page 36], this implies that if the system under consideration is of class C^1 over its associated region, then the existence and uniqueness of the solutions to the initial value problem (I.P.V.) associated with the system are guaranteed. It is evident that the system under study, as given by Eq. (2), is of class C^1. Therefore, based on the aforementioned result, we assume that the solutions to the system (2) exist and are unique.

4   Topological equivalence

To simplify the system by reducing the number of parameters involved and to facilitate both qualitative analysis and numerical simulations, the following change of variables is introduced: $x = uk$, $y = vnk$, and $t = \frac{1}{rk}\tau$. In addition, the parameters are transformed as follows: $A_1 = \frac{m_1}{k}$, $A_2 = \frac{rk}{qn}$, $A_3 = \frac{ark}{q}$, $A_4 = \frac{c}{nk}$,

and $A_5 = \dfrac{s}{rk}$. By applying these transformations to system (2), the following reformulated system is obtained

$$U_\varsigma(u,v): \begin{cases} \dfrac{du}{d\tau} = u(1-u)(u+A_1) - \dfrac{uv}{A_2u+A_3v}, \\[4mm] \dfrac{dv}{d\tau} = v\left(1 - \dfrac{v}{u+A_4}\right)A_5. \end{cases} \tag{9}$$

The system is defined within the following region

$$\bar{\Omega} = \left\{ (u,v) \in \mathbb{R}^2 : 0 < u \leq 1,\ 0 < v \leq 1+A_4 \right\}. \tag{10}$$

This change in the variables induces a diffeomorphism, as demonstrated in [10, 14, 51]. The diffeomorphism is defined by $\varphi : \bar{\Omega} \times \mathbb{R} \to \Omega \times \mathbb{R}$, where $\varphi(u,v,\tau) = (uk, vnk, \dfrac{1}{rk}\tau) = (x,y,t)$. Furthermore, the Jacobian determinant of φ, denoted as $\det(\varphi'(u,v))$, satisfies $\det(\varphi'(u,v)) > 0$. This change of variables ensures that the time orientation is preserved. As a result, the transformed system (9) is topologically equivalent to the original system (2). Notably, this transformation reduces the number of parameters from eight in system (2) to five in system (9). Consequently, the subsequent analysis focuses exclusively on system (9).

5 Critical points

The $u - nullcline$ the system (9) in Ω is

$$v = \frac{uA_2(1-u)(u+A_1)}{1 - A_3(1-u)(u+A_1)},$$

while the $v - nullcline$ in Ω is: $v = u + A_4$. From this, the critical points of the system (9) in its Ω are $(1,0)$, $(0,A_4)$ and (u^*, v^*), where u^* and v^* are determined by the roots of the following polynomial of degree three, which is the result of equating $u - nullcline$ and $v - nullcline$

$$-u^3(A_2+A_3) - u^2(A_3A_4 + (A_1-1)(A_2+A_3)) - u(1 - A_1A_2 + A_3(A_1A_4 - A_1 - A_4)) - A_4(1 - A_1A_3).$$

Following the Cardano method, which provides an analytical solution for any cubic equation (see [13]), the polynomial can first be converted to its normal form by dividing by $-(A_2+A_3)$ and then ordering the terms, yielding

$$u^3 + u^2\left(\frac{A_3A_4 + (A_1-1)(A_2+A_3)}{A_2+A_3}\right) + u\left(\frac{1 - A_1A_2 + A_3(A_1A_4 - A_1 - A_4)}{A_2+A_3}\right) + A_4\left(\frac{1 - A_1A_3}{A_2+A_3}\right).$$

Furthermore, substituting $u = z - (A_3A_4 + (A_1-1)(A_2+A_3))/(A_2+A_3)$, thus eliminating the quadratic term, yields the following form $z^3 + Pz + Q$, where the linear component and its independent term are

defined by

$$P = \frac{1 - A_1 A_2 + A_3(A_1 A_4 - A_1 - A_4)}{A_2 + A_3} - \frac{1}{3}\left(\frac{A_3 A_4 + (A_1 - 1)(A_2 + A_3)}{A_2 + A_3}\right)^2,$$

$$Q = \frac{2}{27}\left(\frac{A_3 A_4 + (A_1 - 1)(A_2 + A_3)}{A_2 + A_3}\right)^3 + A_4\left(\frac{1 - A_1 A_3}{A_2 + A_3}\right)$$

$$- \frac{1}{3}\left(\frac{A_3 A_4 + (A_1 - 1)(A_2 + A_3)}{A_2 + A_3}\right)\left(\frac{1 - A_1 A_2 + A_3(A_1 A_4 - A_1 - A_4)}{A_2 + A_3}\right).$$

Therefore, the critical points of system (9) are given by

$$(u_1, v_1) = (1, 0), \tag{11}$$

$$(u_2, v_2) = (0, A_4), \tag{12}$$

1. A real root ($\Delta > 0$):

$$(u_3, v_3) = (\alpha_1, \beta_1). \tag{13}$$

2. Two real roots ($\Delta = 0$):

$$(u_4, v_4) = (\alpha_2, \beta_2), \tag{14}$$

$$(u_5, v_5) = (\alpha_3, \beta_3), \tag{15}$$

3. Three real roots ($\Delta < 0$):

$$(u_6, v_6) = (\alpha_4, \beta_4), \tag{16}$$

$$(u_7, v_7) = (\alpha_5, \beta_5), \tag{17}$$

$$(u_8, v_8) = (\alpha_6, \beta_6). \tag{18}$$

Here, $\Delta = \left(\dfrac{Q}{2}\right)^2 + \left(\dfrac{P}{3}\right)^3$, $\theta = \arccos\left(\dfrac{3Q}{2P}\sqrt{\dfrac{-3}{P}}\right)$ and $0 < \theta < \pi$. In addition

$$R_1 = \sqrt[3]{\frac{-Q + \sqrt{\Delta}}{2}} + \sqrt[3]{\frac{-Q - \sqrt{\Delta}}{2}} \qquad\qquad , R_2 = 2\sqrt[3]{-\frac{Q}{2}},$$

$$R_3 = -\sqrt[3]{-\frac{Q}{2}} \qquad\qquad\qquad\qquad , R_4 = 2\sqrt{-\frac{P}{3}}\cos\left(\frac{\theta}{3}\right),$$

$$R_5 = 2\sqrt{-\frac{P}{3}}\cos\left(\frac{\theta + 2\pi}{3}\right) \qquad\qquad , R_6 = 2\sqrt{-\frac{P}{3}}\cos\left(\frac{\theta + 4\pi}{3}\right).$$

The main parameters are

$$\alpha_1 = R_1 - \frac{A_3A_4 + (A_1 - 1)(A_2 + A_3)}{3(A_2 + A_3)}, \qquad \beta_1 = \alpha_1 + A_4,$$

$$\alpha_2 = R_2 - \frac{A_3A_4 + (A_1 - 1)(A_2 + A_3)}{3(A_2 + A_3)}, \qquad \beta_2 = \alpha_2 + A_4,$$

$$\alpha_3 = R_3 - \frac{A_3A_4 + (A_1 - 1)(A_2 + A_3)}{3(A_2 + A_3)}, \qquad \beta_3 = \alpha_3 + A_4,$$

$$\alpha_4 = R_4 - \frac{A_3A_4 + (A_1 - 1)(A_2 + A_3)}{3(A_2 + A_3)}, \qquad \beta_4 = \alpha_4 + A_4,$$

$$\alpha_5 = R_5 - \frac{A_3A_4 + (A_1 - 1)(A_2 + A_3)}{3(A_2 + A_3)}, \qquad \beta_5 = \alpha_5 + A_4,$$

$$\alpha_6 = R_6 - \frac{A_3A_4 + (A_1 - 1)(A_2 + A_3)}{3(A_2 + A_3)}, \qquad \beta_6 = \alpha_6 + A_4.$$

The following results ensure that the last six critical points are positive.

Proposition 2. *If $A_3A_4 < (1 - A_1)(A_2 + A_3)$, $1 < A_1A_2$, $A_1A_4 < A_1 + A_4$, $1 < A_1A_3$, $(Q/2)^2 > (P/3)^3$, and $-Q > \sqrt{\Delta}$, then the critical point (u_3, v_3) is positive.*

Proof. Let $A_3A_4 < (1 - A_1)(A_2 + A_3)$, $1 < A_1A_2$, $A_1A_4 < A_1 + A_4$, and $1 < A_1A_3$ it follows that $Q < 0$. However, from $1 < A_1A_2$, $A_1A_4 < A_1 + A_4$ and $A_3A_4 < (1 - A_1)(A_2 + A_3)$ it follows that $P < 0$. From $(Q/2)^2 > (P/3)^3$, it is shown that $\Delta > 0$. Hence, from $-Q + \sqrt{\Delta} > 0$. In addition, from $-Q > \sqrt{\Delta}$ it is deduced that $R_1 > 0$. However, from $A_3A_4 < (1 - A_1)(A_2 + A_3)$, it is clear that

$$\frac{A_3A_4 + (A_1 - 1)(A_2 + A_3)}{3(A_2 + A_3)} < 0.$$

That is $\beta_1 > 0$. Then the critical point (u_3, v_3) is positive. $\qquad\square$

Proposition 3. *If $A_3A_4 < (1 - A_1)(A_2 + A_3)$, $1 < A_1A_2$, $A_1A_4 < A_1 + A_4$, and $1 < A_1A_3$, then the critical point (u_4, v_4) is positive.*

Proof. Let $A_3A_4 < (1 - A_1)(A_2 + A_3)$, $1 < A_1A_2$, $A_1A_4 < A_1 + A_4$, and $1 < A_1A_3$, it follows that $Q < 0$, consequently $R_2 > 0$, and from $A_3A_4 < (1 - A_1)(A_2 + A_3)$ it follows that $\dfrac{A_3A_4 + (A_1 - 1)(A_2 + A_3)}{3(A_2 + A_3)} < 0$, i.e., $\beta_2 > 0$. Then the critical point (u_4, v_4) is positive. $\qquad\square$

Proposition 4. *If $A_3A_4 < (1 - A_1)(A_2 + A_3)$, $1 < A_1A_2$, $A_1A_4 < A_1 + A_4$, and $1 < A_1A_3$, then the critical point (u_5, v_5) is positive.*

Proof. Let $A_3A_4 < (1 - A_1)(A_2 + A_3)$, $1 < A_1A_2$, $A_1A_4 < A_1 + A_4$, and $1 < A_1A_3$, it follows that $Q < 0$, consequently $R_3 > 0$, and from $A_3A_4 < (1 - A_1)(A_2 + A_3)$ it follows that $\dfrac{A_3A_4 + (A_1 - 1)(A_2 + A_3)}{3(A_2 + A_3)} < 0$, i.e., $\beta_3 > 0$. Then the critical point (u_5, v_5) is positive. $\qquad\square$

Proposition 5. *If $1 < A_1A_2$, $A_1A_4 < A_1 + A_4$, and $A_3A_4 < (1 - A_1)(A_2 + A_3)$, then the critical point (u_6, v_6) is positive.*

Proof. Let $1 < A_1A_2$, $A_1A_4 < A_1 + A_4$, it follows that $P < 0$. From the theory, it follows that $0 < \theta < \pi$, then $\cos\left(\dfrac{\theta}{3}\right) \in \langle \frac{1}{2}, 1 \rangle$. Therefore, $R_4 > 0$. Finally, from $A_3A_4 < (1 - A_1)(A_2 + A_3)$, it follows that $\dfrac{A_3A_4 + (A_1 - 1)(A_2 + A_3)}{3(A_2 + A_3)} < 0$, i.e., $\beta_4 > 0$. Then the critical point (u_6, v_6) is positive. $\square$

Proposition 6. *If* $1 < A_1A_2$, $A_1A_4 < A_1 + A_4$, $A_3A_4 < (1 - A_1)(A_2 + A_3)$, *and* $\dfrac{(1 - A_1)(A_2 + A_3) - A_3A_4}{3(A_2 + A_3)} > -R_5$, *then the critical point* (u_7, v_7) *is positive.*

Proof. Let $1 < A_1A_2$ and $A_1A_4 < A_1 + A_4$, it follows that $P < 0$. According to the theory, it is known that $0 < \theta < \pi$, which implies that $\cos\left(\dfrac{\theta + 2\pi}{3}\right) \in \langle -1, -\frac{1}{2} \rangle$. Therefore, it follows that $R_5 < 0$. From the inequality $A_3A_4 < (1 - A_1)(A_2 + A_3)$, we see that

$$\frac{A_3A_4 + (A_1 - 1)(A_2 + A_3)}{3(A_2 + A_3)} < 0.$$

Finally, from the inequality

$$\frac{(1 - A_1)(A_2 + A_3) - A_3A_4}{3(A_2 + A_3)} > -R_5,$$

we deduce that $\alpha_5 > 0$, and consequently, $\beta_5 > 0$. Then the critical point (u_7, v_7) is positive. $\square$

Proposition 7. *If* $1 < A_1A_2$, $A_1A_4 < A_1 + A_4$, $A_3A_4 < (1 - A_1)(A_2 + A_3)$, *and* $\frac{\pi}{2} < \theta < \pi$, *then the critical point* (u_8, v_8) *is positive.*

Proof. Let $1 < A_1A_2$, $A_1A_4 < A_1 + A_4$, it follows that $P < 0$. From the theory, it is salvaged that $\frac{\pi}{2} < \theta < \pi$, then $\cos\left(\dfrac{\theta + 4\pi}{3}\right) \in \langle 0, \dfrac{1}{2} \rangle$. Therefore, $R_6 > 0$. Finally, from $A_3A_4 < (1 - A_1)(A_2 + A_3)$, it follows that $\dfrac{A_3A_4 + (A_1 - 1)(A_2 + A_3)}{3(A_2 + A_3)} < 0$, i.e., $\beta_6 > 0$. Then the critical point (u_8, v_8) is positive. $\square$

6 Local stability analysis

In this section, we analyze the local stability of the critical points. As previously mentioned, system (9) represents a population dynamics model, and our goal is to determine stability results, particularly asymptotic stability. To achieve this, various mathematical tools are available, such as linearization and the Hurwitz criterion, which are applied to the Jacobian matrix. Additionally, methods like LaSalle's Invariance Principle and the generalized Krasovskii Theorem are utilized to analyze the stability of regions containing the critical points. The distinction between these approaches lies in their specific implications for stability analysis. The linearization and the Hurwitz criterion provide conditions for the parameters but not for the initial values. In contrast, LaSalle's Invariance Principle and the generalized Krasovskii Theorem offer conditions for both the parameters and the initial values.

Consequently, the latter two methods allow for a more realistic simulation of the scenario under study compared to the linearization and Hurwitz criterion. However, LaSalle [28,48] and Krasovskii's methods are limited, as they only address the asymptotically stable case. On the other hand, linearization and the Hurwitz criterion encompass both unstable and asymptotically stable cases, enabling a broader range of scenarios to be analyzed. Therefore, the generalized Krasovskii Theorem is used. On the other hand, the

use of Chetaev's Theorem is recommended if instability is to be taken into account, since, like LaSalle and Krasovskii, Chetaev's result acts on a region. The Jacobian of the system (9) is

$$
J = \begin{pmatrix} 2u + A_1 - 2A_1 u - 3u^2 - \dfrac{A_3 v^2}{(A_2 u + A_3 v)^2} & -\dfrac{A_2 u^2}{(A_2 u + A_3 v)^2} \\[4mm] \dfrac{A_5 v^2}{(u + A_4)^2} & A_5 \left(1 - \dfrac{2v}{u + A_4}\right) \end{pmatrix}.
\tag{19}
$$

It should be noted that the stability analysis of the first critical point (11) is not presented because, according to Theorem 4.4, as discussed in [12][page 141], which pertains to the Linearization Theorem using the trace and determinant, this point behaves as a saddle point. Specifically, this is because $\det(J_1) = -A_5(A_1 + 1)$.

6.1 Critical point stability (u_2, v_2)

The criterion of the trace and the determinant is used due to its ease of application. The critical point (12) is substituted into the Jacobian matrix (19), resulting in the following matrix

$$
J_2 = \begin{pmatrix} A_1 - \frac{1}{A_3} & 0 \\ A_5 & -A_5 \end{pmatrix}.
\tag{20}
$$

where the determinant $\det(J_2) = \frac{A_5}{A_3}(1 - A_1 A_3)$ and the trace $trz(J_2) = A_1 - A_5 - \frac{1}{A_3}$

Theorem 2. *If $A_1 A_3 < 1$, and $A_1 < A_5$, then the critical point (u_2, v_2) is asymptotically stable.*

Proof. Let $A_1 A_3 < 1$ so $\det(J_2) > 0$ and from $A_1 < A_5$ it follows that $trz(J_2) < 0$. Then the critical point (u_2, v_2) is asymptotically stable. ☐

The remaining critical points may lead to ecological equilibrium, where all populations survive over time. Therefore, it is essential to present results that ensure these equilibrium points are asymptotically stable. Achieving this result is important because it signifies the system's strong resistance to parameter changes. Numerous tools are available for this purpose, such as linearization and the Routh-Hurwitz criterion. However, these methods often involve exhaustive and complicated mathematical calculations. To simplify the analysis, the Generalized Krasovskii Theorem is employed. Although this theorem requires the use of a pair of symmetric, positive-definite matrices, depending on the system under study, it significantly reduces the mathematical effort. Moreover, the resulting function is bounded according to the conditions of the region around the critical point under analysis.

The Generalized Krasovskii Theorem has been used in control analysis and dynamic systems [24] and is effective in proving the local asymptotic stability of a critical point. It also generates a Lyapunov function suitable for global stability analysis. As stated in [50][page 85], the theorem provides conditions for both the asymptotic local and global stability of a critical point with respect to the system parameters, as well as conditions for the initial value. Additionally, to further facilitate the local stability analysis, the Sylvester criterion [22][page 439] is applied.

6.2   Critical point stability (u^*, v^*)

Due to the nature of the critical points (11)-(16). These lend themselves to be analyzed jointly, i.e., instead of analyzing each of the remaining six critical points, they can be analyzed by $(u^*, v^*) = (\alpha_i, \beta_i)$, where $i = \{1,2,3,4,5,6\}$. To apply the generalized Krasovskii's Theorem to the critical point (u^*, v^*), the symmetric matrices Γ and F are defined on the ball $\mathscr{B}_i = \{(u,v) \in \mathbb{R}^2 : 0 < |u - \alpha_i| < \varepsilon; 0 < |v - \beta_i| < \varepsilon\}$, where $\varepsilon \approx 0$ and $\mathscr{B}_i \subset \bar{\Omega}$:

$$\Gamma = \begin{bmatrix} \dfrac{(A_4 + u)^2 (A_2 u + A_3 v)^2}{u^2} & 0 \\ 0 & \dfrac{(A_4 + u)^2 (A_2 u + A_3 v)^2}{u^2} \end{bmatrix}, \qquad F = \begin{bmatrix} 2A_3 v^2 & A_2 u^2 \\ A_2 u^2 & 0 \end{bmatrix}.$$

Clearly, the matrices Γ and F are positive definite on the ball $\mathscr{B}_i$. Then, the matrix $F(U)$ is

$$F(U) = \begin{bmatrix} 2(A_2 u + A_3 v)^2 M & \dfrac{A_5 v^2 (A_2 u + A_3 v)^2}{(A_4 + u)^2} \\ \dfrac{A_5 v^2 (A_2 u + A_3 v)^2}{(A_4 + u)^2} & -\dfrac{2A_5 (A_2 u + A_3 v)^2 (A_4 + u - 2v)}{A_4 + u} \end{bmatrix},$$

where $M = u(A_1 + u) + u(u - 1) + (A_1 + u)(u - 1)$, before continuing we must clarify that due to the nature of the $\mathscr{B}_i$ ball, we have that $v = u + A_4$ for all $v \in \mathscr{B}_i$. Later, the matrix $F(U)$ can be reduced to

$$F(U) = \begin{bmatrix} 2(A_2 u + A_3 v)^2 M & A_5 (A_2 u + A_3 v)^2 \\ A_5 (A_2 u + A_3 v)^2 & -2A_5 (A_2 u + A_3 v)^2 \end{bmatrix}.$$

Theorem 3. *If $(\alpha_i - \varepsilon)(2A_1 - 1 + 3\alpha_i - 3\varepsilon) \geq A_1 + \alpha_i - \varepsilon$, and $4(\alpha_i - \varepsilon)(2A_1 - 1 + 3\alpha_i - 3\varepsilon) \geq A_5 + A_1 + \alpha_i - \varepsilon$, then the critical point (u^*, v^*) is asymptotically stable.*

Proof. From the theory explained above, the square matrix is $F(U) \in \mathbb{R}^{2 \times 2}$ is negative semidefinite in $\mathscr{B}_i$ if $-F(U)$ is positive semidefinite for all $(u,v) \in \mathscr{B}_i - \{(\alpha_i, \beta_i)\}$. Applying the first part of Sylvester's criterion, we have that the square matrix $-F(U)$ is positive semidefinite for all $(u,v) \in \mathscr{B}_i - \{(\alpha_i, \beta_i)\}$ if all its Principal Minors are nonnegative. Let the matrix

$$-F(U) = \begin{bmatrix} -2(A_2 u + A_3 v)^2 M & -A_5 (A_2 u + A_3 v)^2 \\ -A_5 (A_2 u + A_3 v)^2 & 2A_5 (A_2 u + A_3 v)^2 \end{bmatrix},$$

where its principal minor associates are: $\det(-F(U)(1,1)) = |-2(A_2 u + A_3 v)^2 M|$ and $\det(-F(U)) = A_5 (A_2 u + A_3 v)^4 (4M - A_5)$. From the first condition, it follows that $\det(-F(U)(1,1)) \geq 0$ and from the second condition it follows that $\det(-F(U)) \geq 0$. Therefore, according to Sylvester's criterion, the matrix $-F(U)$ is positive semidefinite for all $(u,v) \in \mathscr{B}_i$. That is, the matrix $F(U)$ is negative semidefinite . Then according to the generalized Krasovskii Theorem, the critical point (u^*, v^*) is asymptotically stable. $\qquad \square$

7 Global stability analysis

This type of analysis strengthens and extends the results obtained from the local stability analysis. Specifically, it ensures that the conclusions drawn from local stability hold across the entire region associated with the system. The following demonstrates that the behavior of the vector field, as in [29, 38], $U_\varsigma(u,v)$ (9) in the region (10) is globally asymptotically stable. According to the generalized Krasovskii Theorem, we have $V(x) = U_\varsigma(u,v)^T \Gamma U_\varsigma(u,v)$, that is,

$$V(u,v) = A_5{}^2 v^2 (A_2 u + A_3 v)^2 \left(1 - \frac{v}{u+A_4}\right)^2 + u^2 (A_2 u + A_3 v)^2 \left((1-u)(A_1+u) - \frac{v}{A_2 u + A_3 v}\right)^2.$$

Because the trend of $\frac{v}{u+A_4}$ is not clear, when $||(u,v)|| \to \infty$, the L'Hôpital rule applies. It turns out that $\lim \frac{v}{u+A_4} = 1$, when $||(u,v)|| \to \infty = 1$. Putting this last result in $V(u,v)$, it follows that $V(u,v) \to \infty$ when $||(u,v)|| \to \infty$. By the second part of the generalized Krasovskii Theorem, the vector field $U_\sigma(u,v)$ (2) in the region (10) is globally asymptotically stable.

8 Periodic solutions

Periodic solutions, also known as periodic orbits or closed orbits in population dynamics, are crucial for understanding how species populations interact and evolve in cyclically changing environments. One important application of periodic solutions is bifurcation analysis. Bifurcations refer to phenomena in which a dynamical system exhibits periodic solutions near an equilibrium point.

In population dynamics, this is significant as it can indicate changes in the stability of populations under varying environmental conditions. To search for periodic solutions in the system (2), the Dulac criterion, as discussed in [14, page 102], is employed. This criterion utilizes a Φ function, known as the Dulac function, which is difficult to determine due to its lack of clear constraints, making it any smooth function. To address this challenge, a construction technique for the Dulac function is provided in [41, pages 44-45], [43, page 3], and [42, page 3]. Take Section 2.4 of [44] as an example. The following candidate function is defined as a Dulac function: $\Phi = (uv)^{-1}$. It is clear that as in the local stability analysis section, one can check for the existence or not of periodic solutions at the critical points (11)-(16). Using the critical point (u^*, v^*).

Theorem 4. *If* $\alpha_i > \varepsilon$, $\beta_i > \varepsilon$, *and* $\dfrac{A_2}{C_i} > \dfrac{D_i}{(\beta_i - \varepsilon)(\alpha_i - \varepsilon)}$, *then there are no periodic solutions in* $\mathscr{B}_i$, *where* $C_i = (A_2(\alpha_i + \varepsilon) + A_3(\beta_i + \varepsilon))^2$, $D_i = A_5 + (\alpha_i - \varepsilon)(2\alpha_i + 2\varepsilon + A_1 - 1)$.

Proof. Let $\alpha_i > \varepsilon$ and $\beta_i > \varepsilon$. Then, the function Φ is smooth on the ball $\mathscr{B}_i$ which is simply connected. Then, from the ball $\mathscr{B}_i$ we obtain $\alpha_i - \varepsilon < u < \alpha_i + \varepsilon$, $\beta_i - \varepsilon < v < \beta_i + \varepsilon$. From

$$\frac{A_2}{C_i} > \frac{D_i}{(\beta_i - \varepsilon)(\alpha_i - \varepsilon)},$$

it is clear that $0 < div(\Phi.U_\varsigma(u,v))$, $forall(u,v) \in \mathscr{B}_i$. Then according to Dulac's criterion, there are no periodic orbits in $\mathscr{B}_i$. $\qquad\square$

9 Numerical analysis

Computational simulations play a fundamental role in mathematical modeling applied to ecology, enabling the exploration of complex dynamics in natural systems that would be difficult or impossible to analyze solely through analytical methods. These tools provide an efficient means to evaluate diverse scenarios, conduct virtual experiments, and analyze model sensitivity to key parameters, which is essential for understanding nonlinear ecological interactions, spatiotemporal processes, and emergent behaviors. Furthermore, simulations facilitate the integration of empirical data, allowing for more realistic predictions and quantification of uncertainty associated with models. This not only enhances the accuracy of theoretical insights but also strengthens their applicability in decision-making for the conservation and sustainable management of ecosystems.

In this section, we present the numerical analysis of the critical points that satisfy the previously proposed conditions. The analysis involves the interpretation of simulations performed for each critical point, utilizing several Python programming packages, such as SciPy, Matplotlib, and SymPy. The simulations are carried out in Google Colab, a free cloud-based platform that enables users to write, run, and share Python code. The simulations are implemented on the differentially equivalent system, specifically on (9). The predefined *odeint* function from the *integrate* module of the SciPy package is used to solve the system. This function helps accurately represent the temporal evolution of the populations and ensures more precise simulations. Additionally, the *Sympy* package is used to handle complex numerical calculations, including local and global stability analyses, as well as determining the correct values for each parameter and initial condition.

9.1 Numerical analysis the critical point (u_6, v_6)

The simulation (1) is conditioned by Proposition 5 and Theorem 3. The initial point is taken to be $(u_6, v_6) = (0.66420, 1.16420)$, $A_1 = 0.7$, $A_2 = 1.8$, $A_3 = 0.9$, $A_4 = 0.5$, $A_5 = 0.8$. By replacing, we have: $P = -0.38555555555555554$, $Q = 0.0514705075445816$, $\Delta = -0.0014604383177060103$, $\alpha_4 = 0.6642073686614601$, $\beta_4 = 1.1642073686614602$, $\varepsilon = 10^{-5}$, $\theta = 1.5805454180680192$ (in radians).

(a) Populations vs. time **(b)** Prey vs. predator
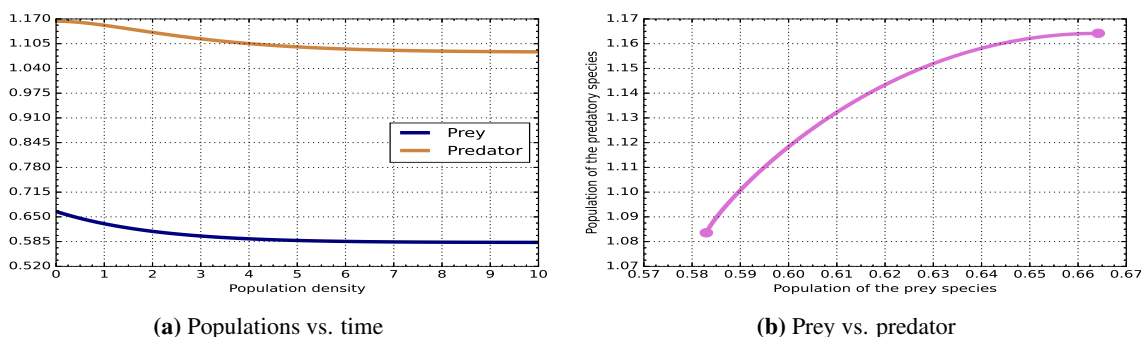
Figure 1: Simulation in the coexistence state at point u_6 and v_6 (first stage)

Figure 1a, simulates the population dynamics of the prey species divided into two phases. The first phase occurs over a shorter period, during which the prey population declines steadily. As the population stabilizes, it transitions into the second phase, where the prey population remains practically constant with only minor fluctuations, maintaining a minimum level without going extinct. Simultaneously, the

predator species also undergoes a two-phase population dynamic. Similar to the prey species, the predator population decreases during the first phase, experiencing losses over a similar time frame. Once it stabilizes, the predator population enters the second phase, where it remains largely unchanged, keeping its population at a minimum level without extinction.

Figure 1b, illustrates the population dynamics of the predator species, which decrease quadratically in relation to the population dynamics of the prey species. Both species experience a decline in three distinct phases. The first phase begins with the initial values of the simulation, $(0.66420, 1.16420)$, where the prey species suffers greater losses than the predator species. In the second phase, both species experience nearly the same rate of decline, which is most noticeable in the more linear section of the graph. Finally, in the third phase, the predator species declines at a faster rate than the prey species. Despite these fluctuations, neither species goes extinct.

The simulation (2), is conditioned by Proposition 2, and the Theorem 3. The initial point is taken to be $(0.79119, 0.89119)$, $A_1 = 0.8$, $A_2 = 1.3$, $A_3 = 2.5$, $A_4 = 0.1$, $A_5 = 0.9$. Replacing we have: $P = -0.5560041551246536$, $Q = -0.051100123924770355$, $\Delta = -0.005713248760556907$, $\alpha_4 = 0.791194444563359$, $\beta_4 = 0.891194444563359$, $\varepsilon = 10^{-5}$, $\theta = 1.5652072971566442$ (in radians).

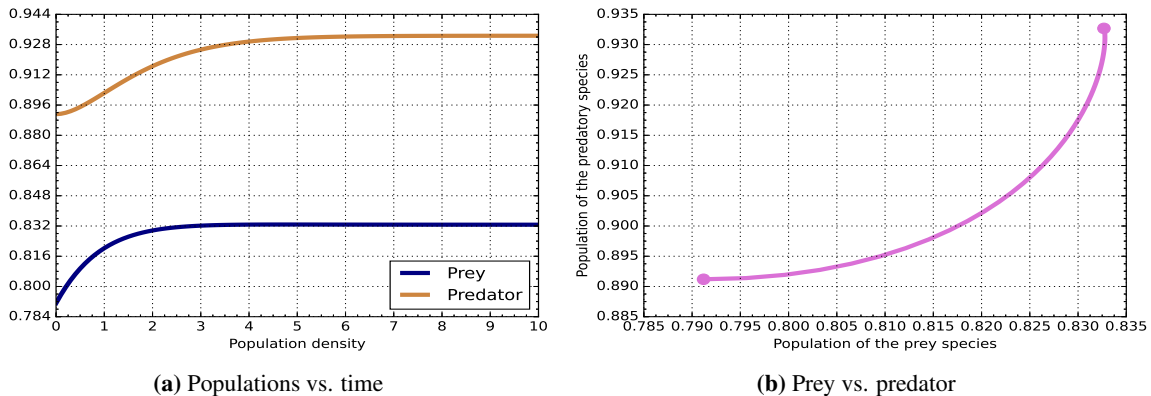**(a)** Populations vs. time

(b) Prey vs. predator

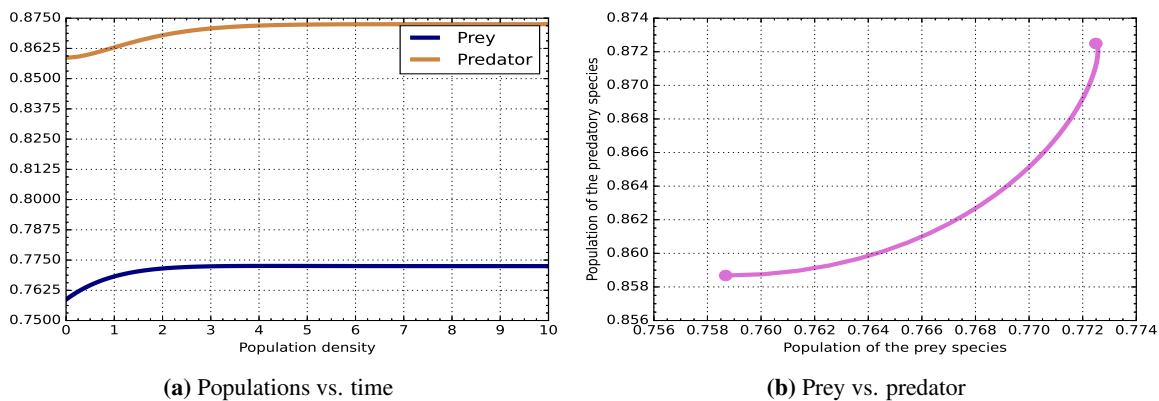**Figure 2:** Simulation in the coexistence state at point u_6 and v_6 (second stage)

Figure 2a, simulates the population dynamics of the prey species are divided into two phases. In the first, shorter phase, the prey population experiences a steady increase, which eventually stabilizes as it enters the second phase. During this second phase, the prey population remains nearly constant, with only minor fluctuations, stabilizing at its maximum possible size. Similarly, the predator species also undergoes two phases of population dynamics. The behavior of the predator species mirrors that of the prey. In the first phase, the predator population increases logarithmically, over a slightly longer period than the prey's first phase, and then stabilizes. In the second phase, the predator population undergoes minimal change, remaining constant at its maximum possible size for the remainder of the time.

Figure 2b, ilustrates the population dynamics of the predator species grow exponentially in relation to the prey species. Both species experience growth in three phases. The first phase begins with the initial values of the simulation $(0.79119, 0.89119)$, during which the prey species grows faster than the predator species. In the second phase, both species grow at nearly the same rate, which is reflected in the linear portion of the graph. Finally, in the third phase, the predator species increases in population more

rapidly than the prey species, until both species reach their maximum possible population sizes.

The simulation (3), is conditioned by Proposition 2, and Theorem 3. The initial point is taken to be $(0.75868, 0.85868)$, $A_1 = 0.9$, $A_2 = 1.5$, $A_3 = 1.3$, $A_4 = 0.1$, $A_5 = 1.1$. By replacing we have $P = -0.5484566326530613$, $Q = -0.015859602769679303$, $\Delta = -0.006047426425106079$, $\alpha_4 = 0.7586879402151852$, $\beta_4 = 0.8586879402151851$, $\varepsilon = 10^{-5}$, $\theta = 1.5652072971566442$ (in radians).

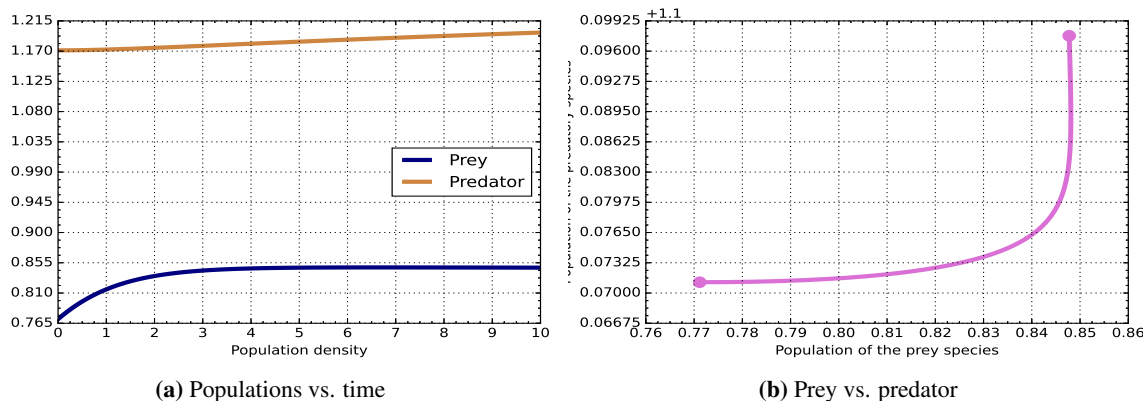**(a)** Populations vs. time   **(b)** Prey vs. predator

Figure 3: Simulation in the coexistence state at point u_6 and v_6 (third stage)

Figure 3a, simulates the population dynamics of the prey species are divided into two phases. The first phase, which is shorter than the second, sees the prey species experiencing a constant population increase, eventually stabilizing as it enters the second phase. In this second phase, the prey population stabilizes, with the number of individuals undergoing only small changes and remaining practically constant at its maximum possible population size. Meanwhile, the predator species also experiences population dynamics divided into two phases. The behaviour of the predator species mirrors that of the prey species. In the first phase, the predator population increases logarithmically over a period slightly longer than the first phase of the prey species, before stabilizing. In the second phase, the predator species experiences very little change, and its population remains constant at its maximum possible level for the rest of the time.

Figure 3b, ilustrates the population dynamics of the predator species grow exponentially in relation to the population dynamics of the prey species. Specifically, both species experience an increase in three distinct phases. The first phase begins with the initial values of this simulation $(0.75868, 0.85868)$, where the prey species grows at a faster rate than the predator species. In the second phase, both species grow at nearly the same rate, which is reflected in the most linear portion of the graph. Finally, in the third phase, the predator species outpaces the prey species in growth, eventually reaching the maximum possible population size for both species.

The simulation (4), is conditioned by Proposition 2, and Theorem 3. The initial point is taken to be $(0.77116, 1.17116)$, $A_1 = 0.5$, $A_2 = 2.5$, $A_3 = 3.1$, $A_4 = 0.4$, $A_5 = 0.05$. By replacing we have $P = -0.4580102040816327$, $Q = -0.08101457725947521$, $\Delta = -0.0019176163637932505$, $\alpha_4 = 0.7711600073781018$, $\beta_4 = 1.1711600073781017$, $\varepsilon = 10^{-5}$, $\theta = 1.5589443754223917$ (in radians).

(a) Populations vs. time

(b) Prey vs. predator

Figure 4: Simulation in the coexistence state at point u_6 and v_6 (fourth stage)

Figure 4a, simulates the population dynamics of the prey species are divided into two phases. The first phase, which lasts for a shorter period than the second, sees the prey species experiencing a constant population increase. As it transitions into the second phase, the prey population stabilizes, with the number of individuals undergoing small changes and remaining practically constant at its maximum possible population size. Meanwhile, the predator species undergoes a single-phase population dynamic. During this phase, the predator population increases constantly in a linear fashion, eventually stabilizing and remaining at its maximum possible population size. Figure 4b, ilustrates the population dynamics of the predator species grow exponentially in relation to the population dynamics of the prey species. This results in the populations of both species increasing in three phases. The first phase begins with the initial values of this simulation $(0.77116, 1.17116)$, where the prey species grows faster than the predator species. In the second phase, both species grow at nearly the same rate, which is evident in the most linear section of the graph. Finally, in the third phase, the predator species grows faster than the prey species, eventually reaching the maximum possible population size for both species.

10   Conclusions

The objective of this study was to examine the intricate ecological dynamics of an ecosystem consisting of a prey species, which serves as the primary food source for a predator species. The prey population growth is constrained by the carrying capacity of the environment, determined by the availability of resources in the ecosystem. At low population densities, the prey exhibits a positive density-dependent growth rate, influenced by cooperative behaviors such as social interactions that enhance survival and reproduction. The predator population, in turn, is regulated by the availability of prey, with the addition of an alternative food source introducing further complexity into the system. The dynamics of this system are modeled using a two-dimensional system of ordinary differential equations (ODEs). The analysis begins by establishing fundamental properties of the model, including the positivity, boundedness, existence, and uniqueness of solutions. The system is shown to possess eight equilibrium points: two on the coordinate axes and six resulting from the intersections of the isoclines. To simplify the analysis, a topologically equivalent reduced system is derived, involving three fewer parameters than the original. Key mathematical tools are employed to assess the stability of the equilibrium points. These include the trace-determinant criterion, LaSalle's Invariance Principle, the generalized Krasovskii theorem, and

the Dulac–Bendixson criterion. Conditions are derived to ensure local and global asymptotic stability, providing explicit relationships between model parameters and initial population values. Numerical simulations were conducted to explore scenarios meeting these stability conditions. For the single favorable case simulated, it was observed that:

- From the Figure 1a of the simulation (1), it is observed that both species experience a population decline until stabilizing at a minimum viable population size, avoiding extinction for either species. Similarly, the second Figure 1b of the simulation (1) shows that the populations of both species decrease quadratically without reaching the origin. Consequently, based on the simulation (1), it can be concluded that the critical point $(u6, v6)$ represents a stable ecological equilibrium. This implies that neither species becomes extinct over time, highlighting the persistence of both populations in the ecosystem.

- From the Figure 2a of the simulation (2), it is observed that both species experience population growth until stabilizing at their maximum possible population sizes, constrained by the system's ecological parameters. Similarly, the second Figure 2b of the simulation (2) indicates exponential growth of both species before stabilization. Consequently, based on the simulation (2), it can be concluded that the critical point $(u6, v6)$ represents a stable ecological equilibrium. This suggests that neither species faces extinction over time, with both populations persisting and thriving within the ecosystem.

- From the Figure 3a of the simulation (3), it is observed that both species experience population growth until stabilizing at their maximum attainable population sizes, as determined by the ecological parameters of the system. Similarly, the second Figure 3b of the simulation (3) illustrates exponential growth of both species before reaching stabilization. Consequently, based on the simulation (3), it can be concluded that the critical point $(u6, v6)$ represents a stable ecological equilibrium. This result implies that neither species faces extinction over time, with both populations persisting and coexisting in the ecosystem.

- From the Figure 4a of the simulation (4), it is observed that both species grow until stabilizing at their maximum feasible population sizes, as dictated by the system's ecological parameters. Similarly, the second Figure 4b of the simulation (4) shows exponential growth of both species prior to stabilization. Consequently, based on the simulation (4), it is concluded that the critical point $(u6, v6)$ represents a stable ecological equilibrium. This result indicates that neither species goes extinct over time, and both populations persist and coexist sustainably within the ecosystem.

- It is also concluded that, among the four cases presented of population dynamics versus time, three exhibit permanent growth until reaching a maximum feasible population size (2a), (3a), (4a), while only one case shows a population decline stabilizing at the minimum viable population size without extinction for either species (1a). Additionally, two of the cases of permanent growth exhibit very similar behavior (2a), (3a). From this analysis, it can be inferred that the predator and prey species modeled in this study tend to grow until reaching a maximum sustainable population size, as determined by the ecological constraints of their environment. Furthermore, their population dynamics in certain cases align closely with those observed in the simulations (2a) and (3a).

- It is also concluded that, among the four cases presented of population versus population dynamics, three exhibit exponential growth (2b), (3b), (4b), while one case demonstrates quadratic decline

(1b). From this, it can be inferred that the predator and prey species described by the model generally exhibit rapid growth under most ecological conditions considered.

Furthermore, it is concluded that the system does not admit periodic solutions. Based on the four favourable cases for ecological balance, it is determined that the model achieves biological equilibrium. This implies that the interacting populations in the proposed scenario persist over time, maintaining their coexistence without extinction. However, despite the modifications introduced, models of this type have inherent limitations. From experimental studies, such as those by [17], it is evident that Holling's type II functional response can be applied across a wide range of ecological scenarios. Nonetheless, its effectiveness is particularly notable when modeling populations of invertebrates and small vertebrates. It is recommended that, while incorporating perturbations such as the mixed functional response (which is rate-dependent), this line of research should be continued, emphasizing the role of the weak Allee effect. This effect highlights the critical importance of social behavior in driving population growth at low densities, a phenomenon especially prominent in invertebrates.

For future research, the weak Allee effect could be replaced by the strong Allee effect, or even extended to incorporate a double Allee effect. This extension could account for ecological factors such as predator cannibalism, prey defensive strategies (e.g., group defense, shelter-seeking), or the indirect fear effects experienced by prey. Furthermore, this ecological model could be adapted into an eco-epidemiological framework by employing delay differential equations or partial differential equations instead of ordinary differential equations. These proposed adjustments are relevant not only to the system under study but also to the foundational models upon which this study is based. Additionally, for future investigations into periodic solutions, it would be worthwhile to explore scenarios where such solutions exist, examining both local and global bifurcations in one- and two-dimensional systems.

Acknowledgments

References

[1] H.R. Akcakaya, R. Arditi, L.R. Ginzburg, *Ratio-dependent predation: An abstraction that works*, Ecology **76** (1995) 995-1004.

[2] W.C. Allee, *Animal aggregations*, The Quarterly Review of Biology **2** (1927) 367–398.

[3] W.C. Allee, E.S. Bowen, *Studies in animal aggregations: Mass protection against colloidal silver among goldfishes*, Journal of Experimental Zoology **61** (1932) 185–207.

[4] R. Arditi, L.R. Ginzburg, *Coupling in predator-prey dynamics: ratio-dependence*, J. Theor. Biol. **139** (1989) 311–326.

[5] R. Arditi, L.R. Ginzburg, H.R. Akcakaya, *Variation in plankton densities among lakes: A case for ratio-dependent Predation Models*, The American Naturalist **138** (1991) 1287-1296.

[6] E.A. Barbašin, N.N. Krasovskiĭ, *On stability of motion in the large*, Doklady Akad. Nauk SSSR (N.S.) **86** (1952) 453–456 (in Russian).

[7] C. Cosner, D.L. DeAngelis, J.S. Ault, D.B. Olsen, *Effects of spatial grouping on the functional response of predators*, Theor. Pop. Biol. **56** (1999) 65–75.

[8] I. Bashkirtseva, L. Ryashko, *Noise-induced shifts in the population model with a weak Allee effect*, Phys. A **491** (2018) 28–36.

[9] I. Bashkirtseva, T. Perevalova, *Analysis of stochastic bifurcations in the eco-epidemiological oscillatory model with weak Allee effect*, Internat. J. Bifur. Chaos Appl. Sci. Engrg. **32** (2022) Paper No. 2250124, 14.

[10] R. Benazic, *Tópicos de Ecuaciones Diferenciales Ordinarias*, UNI, Perú, 2007.

[11] L. Berec, E. Angulo, F. Courchamp, *Multiple Allee effects and population management*, Trends in Ecology & Evolution **22** (2006) 185–191.

[12] F. Brauer, C. Castillo-Chavez, *Mathematical Models in Population Biology and Epidemiology*, Texts in Applied Mathematics, Springer, New Yor, 2012.

[13] G. Cardano, *Ars Magna or the Rules of Algebra*, Dover Publications, Inc., New York, 1993.

[14] C. Chicone, *Ordinary Differential Equations with Applications*, Springer, New York, 2006.

[15] F. Courchamp, L. Bereck, J. Gascoigne, *Allee Effects in Ecology and Conservation*, Oxford University Press, 2008.

[16] C. Egami, *Positive periodic solutions of nonautonomous delay competitive systems with weak Allee effect*, Nonlinear Anal. Real World Appl. **10** (2009) 494–505.

[17] V. Fernández-Arhex, J.C. Corley, *La respuesta funcional: una revisión y guía experimental*, Ecología austral **14** (2004) 83–93.

[18] J.D. Ferreira, C.A.T. Salazar, P.C.C. Tabares, *Weak Allee effect in a predator-prey model involving memory with a hump*, Nonlinear Anal. Real World Appl. **14** (2013) 536–548.

[19] E. González-Olivares, A. Rojas-Palma, *Colaboración entre depredadores y efecto Allee débil en las presas. Consecuencias sobre la dinámica de un modelo de depredación*, Selecciones Matemáticas **9** (2022) 173–183.

[20] A.P. Gutierrez, *Physiological basis of ratio-dependent predator-prey theory: The metabolic pool model as a paradigm.*, Ecology **73** (1992) 1552-1563.

[21] L. Hanski, *The functional response of predators: worries about scale*, Trends. Ecol. Evol. **6** (1991) 141–142.

[22] R.A. Horn and C.R. Johnson, *Matrix analysis*, Cambridge University Press, 2013.

[23] Sze-Bi Hsu, *Ordinary Differential Equations with Applications*, World Scientific Publishing Co. Pte. Ltd., Hackensack, NJ, 2013.

[24] J. Pérez–Núñez, *Análisis y simulación de un modelo matemático glucosa-insulina en personas con diabetes tipo I*, Ph. D. Thesis, UNMSM, Lima, Perú, 2017.

[25] J. Pérez–Núñez et al., *A mathematical model the transmission dynamics of tuberculosis with exogenous reinfection in the infection-free state*, Int. J. Appl. Eng. Technol. **4** (2022) 38–45.

[26] X. Jia, K. Huang, C. Li, *Bifurcation analysis of a modified Leslie-Gower predator-prey system*, Internat. J. Bifur. Chaos Appl. Sci. Engrg. **33** (2023) Paper No. 2350024, 24.

[27] A. Kramer, L. Berec, J.M. Drake, *Allee effects in ecology and evolution*, J. Anim. Ecol. **87** (2018) 7–10.

[28] J.P. LaSalle, *Some extensions of liapunov's second method*, IRE Transactions on Circuit Theory **CT-7** (1960) 520–527.

[29] O. Lazaar, M. Serhani, *Stability and optimal control of a prey-predator model with prey refuge and prey infection*, Int. J. Dyn. Control **11** (2023) 1934–1951.

[30] P.H. Leslie, *Some further notes on the use of matrices in population mathematics*, Biometrika **35** (1948) 213–245.

[31] C. Liang, H.F. Huo, H. Xiang, *Modelling mosquito population suppression based on competition system with strong and weak Allee effect*, Math. Biosci. Eng. **21** (2024) 5227–5249.

[32] M. Liermann, R. Hilborn, *Depensation: evidence, models and implications*, Fish and Fisheries **2** (2001) 33–58.

[33] R. Lin, S. Liu, X. Lai, *Bifurcations of a predator-prey system with weak Allee effects*, J. Korean Math. Soc. **50** (2013) 695–713.

[34] T. Liu, L. Chen, F. Chen, Z. Li, *Dynamics of a Leslie-Gower model with weak Allee effect on prey and fear effect on predator*, Internat. J. Bifur. Chaos Appl. Sci. Engrg. **33** (2023) Paper No. 2350008, 19.

[35] A.J. Lotka, *Elements of Physical Biology*, Williams & Wilkins, Baltimore: Waverly, 1925.

[36] D. Luo, Q. Wang, *Global dynamics of a Beddington-DeAngelis amensalism system with weak Allee effect on the first species*, J. Appl. Math. Comput. **68** (2022) 655–680.

[37] T. Ma, X. Meng, *Global stability analysis and Hopf bifurcation due to memory delay in a novel memory-based diffusion three-species food chain system with weak Allee effect*, Math. Methods Appl. Sci. **47** (2024) 6079–6096.

[38] V. Madhusudanan, S. Vijaya, *Dynamical Behaviour in Two Prey-Predator System with Persistence*, Bull. Math. Anal. Appl. **16** (2016) 20–37.

[39] T.R. Malthus, *An Essay on the Principle of Population*, Penguin Classics, London, 1798.

[40] R.M. May, *Stability and Complexity in Model Ecosystems*, Princeton university press, 2001.

[41] O. Osuna, G. Villaseñor, *On the Dulac functions*, Qual. Theory Dyn. Syst. **10** (2011) 43–49.

[42] O. Osuna, G. Villaseñor, *Some properties theDulac functions set*, Electron. J. Qual. Theory Differ. Equ. **2011** (2011) No. 72, 8.

[43] O. Osuna, C. Vargas-De-León, *Construction of Dulac functions for mathematical models in population biology*, Int. J. Biomath. **8** (2015) 1550035, 20.

[44] N.P. Romero, C.U. Fernández, *Mathematical model of a predator-prey food chain: plankton-anchovy*,Rev. Mat. **29** (2022) 69–103.

[45] M. Romero–Ordoñez and J. Pérez–Núñez and L. Vásquez–Serpa, *Análisis cualitativo y simulaciones de un modelo depredador–presa tipo May–Holling–Tanner rázon–dependiente con una fuente alternativa de alimento para el depredador*, Sel. Mat. **9** (2022) 196–209.

[46] K. Sarkar, S. Khajanchi, P.C. Mali, *A delayed eco-epidemiological model with weak Allee effect and disease in prey*, Internat. J. Bifur. Chaos Appl. Sci. Eng. **32** (2022) Paper No. 2250122, 26.

[47] S.K. Sasmal, J. Chattopadhyay, *An eco-epidemiological system with infected prey and predator subject to the weak Allee effect*, Math. Biosci. **246** (2013) 260–271.

[48] S. Sastry, *Nonlinear Systems*, Springer-Verlag, New York, 1999.

[49] S. Sharma, G.P. Samanta, *A ratio-dependent predator-prey model with Allee effect and disease in prey*, J. Appl. Math. Comput. **47** (2015) 345–364.

[50] J.J. Slotine and W. Li, *Applied Nonlinear Control*, Prentice-Hall, 1991.

[51] J. Sotomayor, *Lições de Equações Diferenciais Ordinárias*, Instituto de Matemática Pura e Aplicada, Rio de Janeiro, 1979.

[52] P.A. Stephens, W.J. Sutherland, R.P. Freckleton, *What is the Allee effect?*, Oikos **87** (1999) 185–190.

[53] P.C. Tabares, J.D. Ferreira, V. Rao, *Weak Allee effect in a predator-prey system involving distributed delays*, Comput. Appl. Math. **30** (2011) 675–699.

[54] P. Turchin, *Complex Population Dynamics: A Theoretical/Empirical Synthesis*, Monographs in Population Biology, Princeton University Press, Princeton, NJ, 2003.

[55] P.-F. Verhulst, *Notice sur la loi que la population suit dans son accroissement*, Correspondence mathematique et physique **10** (1838) 113–129.

[56] S. Valenzuela-Figueroa, E. González-Olivares, A. Rojas-Palma, *Influence of the weak Allee effect on prey in a Leslie-Gower type predation model with sigmoid functional response*, Rev. Mat. **29** (2022) 105–138.

[57] V. Volterra, *Fluctuations in the abundance of a species considered mathematically*, Nature **118** (1926) 558–560.

[58] M.H. Wang, M. Kot, *Speeds of invasion in a model with strong or weak Allee effects*, Math. Biosci. **171** (2001) 83–97.

[59] Y. Wang, J. Shi, *Persistence and extinction of population in reaction-diffusion-advection model with weak Allee effect growth*, SIAM J. Appl. Math. **79** (2019) 1293–1313.

[60] W. Wu, Y. Ye, *Existence and stability of almost periodic solutions of nonautonomous competitive systems with weak Allee effect and delays*, Commun. Nonlinear Sci. Numer. Simul. **14** (2009) 3993–4002.

[61] L. Zhang, Y. Xu, G. Liao, *Codimension-two bifurcations and bifurcation controls in a discrete biological system with weak Allee effect*, Internat. J. Bifur. Chaos Appl. Sci. Eng. **32** (2022) Paper No. 2250036, 27.

[62] Q. Yang, X. Zhang, D. Jiang, M. Shao, *Analysis of a stochastic predator-prey model with weak Allee effect and Holling-$(n+1)$ functional response*, Commun. Nonlinear Sci. Numer. Simul. **111** (2022) Paper No. 106454, 18 pp.

[63] L. Zhao, J. Shen, *Relaxation oscillations in a slow-fast predator-prey model with weak Allee effect and Holling-IV functional response*, Commun. Nonlinear Sci. Numer. Simul. **112** (2022) Paper No. 106517, 19 pp.